Supplementary Material

The dipole potential correlates with lipid raft markers in the plasma membrane of living cells

Tamás Kovács, Gyula Batta, Florina Zákány, János Szöllősi, Peter Nagy

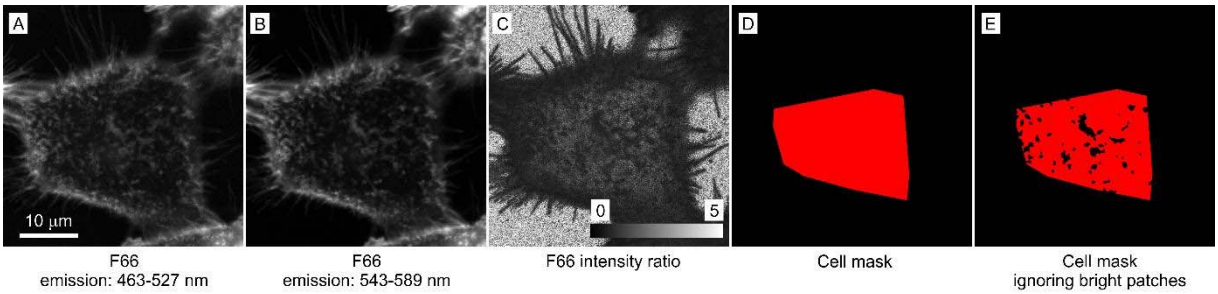

Supplemental Figure S1. Representative images showing staining of cells with the dipole potential-sensitive indicator, F66. A431 cells were treated with Pluronic F-127 followed by staining with F66. The dye was excited at 405 nm, and its emission was measured in two wavelength ranges, 463-527 nm ("blue channel", A) and 543-589 nm ("green channel", B). An emission ratio image was calculated by dividing the intensity recoded in the blue channel by the intensity in the green channel on a pixel-by-pixel basis (C). The ratio values were only evaluated in a mask, drawn manually, corresponding to the flat membrane adjacent to the coverslip (D) or within this cell mask ignoring the brightest patches (E).

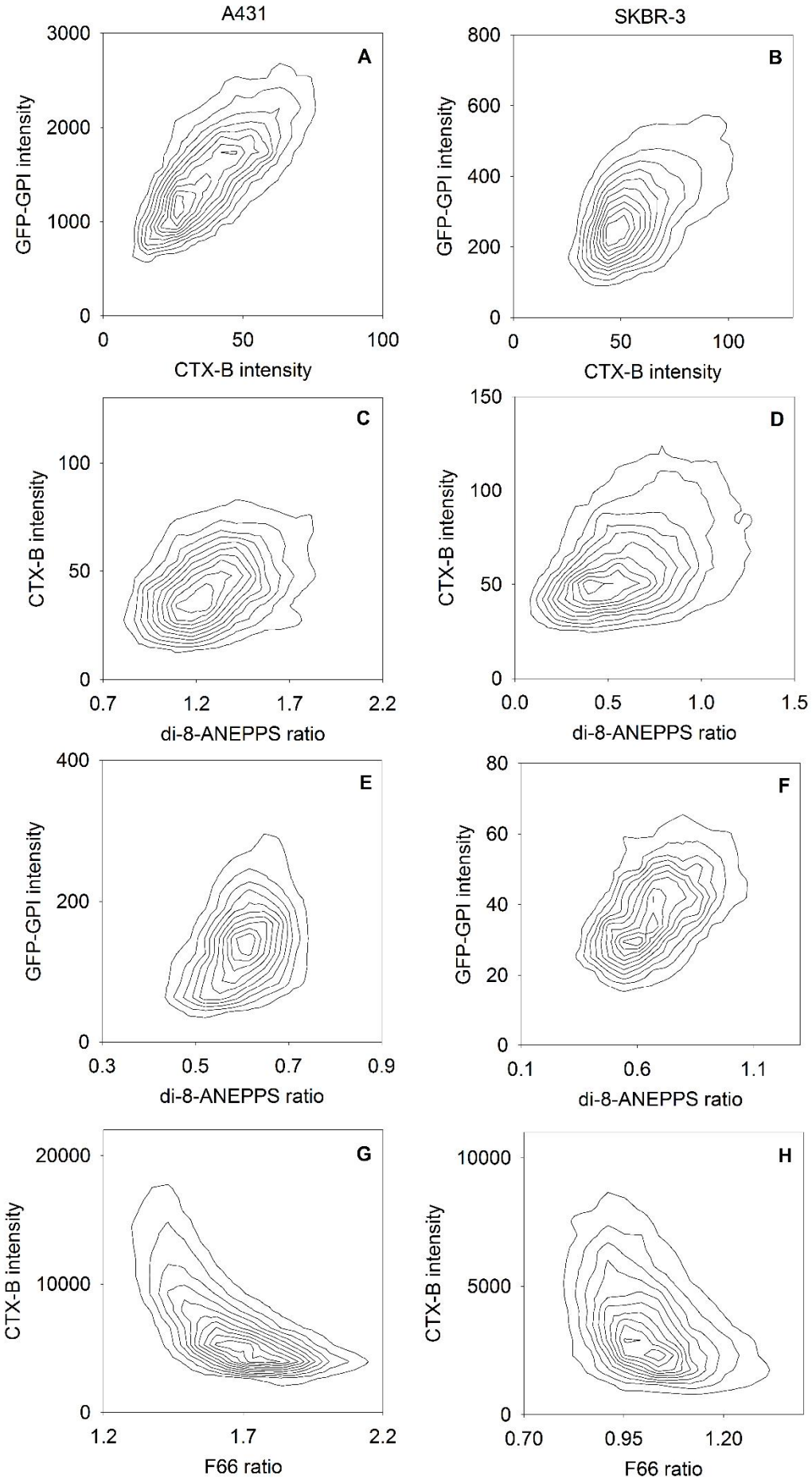
A431
SKBR-3
A
B
C
D
E
F
G
H
GFP-GPI intensity
CTX-B intensity
di-8-ANEPPS ratio
F66 ratio
3000
2000
1000
0
50
100
800
600
400
200
150
0.0
0.5
1.0
1.5
0.7
1.2
1.7
2.2
0.3
0.9
80
60
40
20
0.1
0.6
1.1
20000
10000
5000
0.70
0.95
1.20

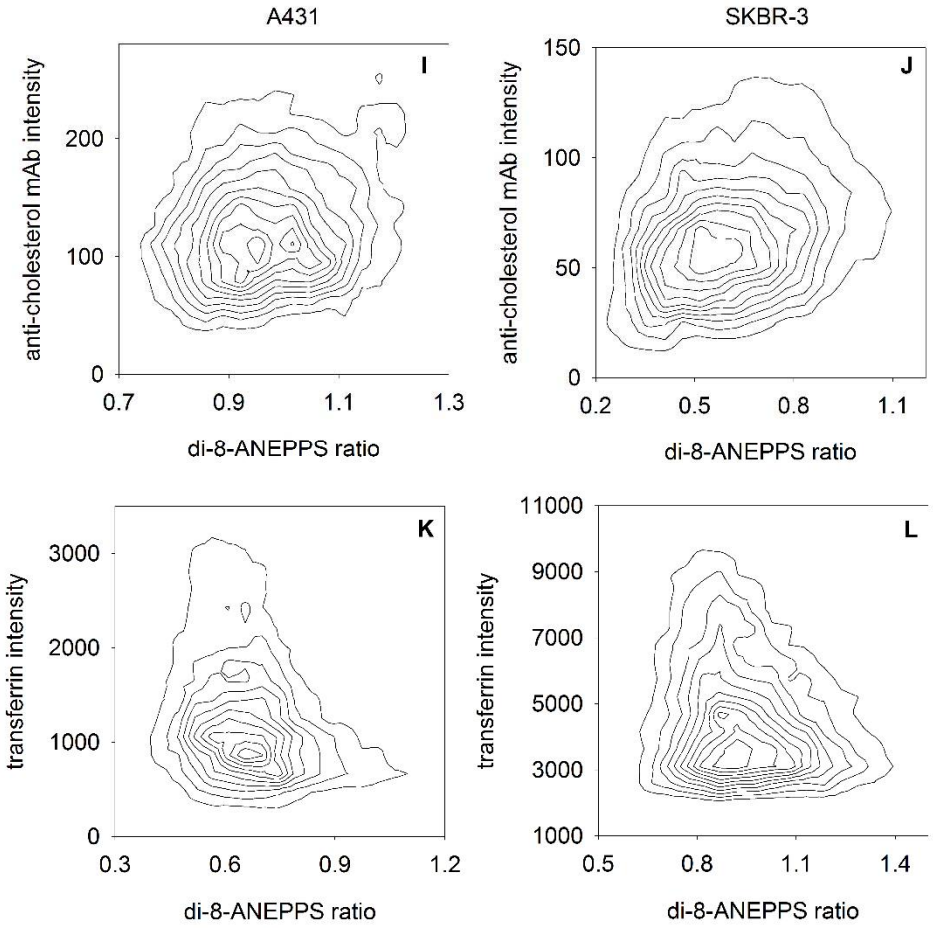

Supplemental Figure S2. Representative contour plots showing the correlation between the dipole potential and lipid raft markers. **A-B.** A431 (A) and SKBR-3 (B) cells were transfected with GFP-GPI followed by labeling them with AlexaFluor647-CTX-B two days after transfection. The correlation of the intensity of the two lipid raft markers are displayed. **C-L.** A431 (C, E, G, I, K) and SKBR-3 (D, F, H, J, L) cells were labeled with di-8-ANEPPS (C-F, I-L) or F66 (G, H) to measure their dipole potential. Transfection with GFP-GPI (E, F), labeling with AlexaFluor647-CTX-B (C, D, G, H) or with anti-cholesterol mAb (I, J) was used as a lipid raft marker. Alternatively, non-raft membrane domains were labeled with AlexaFluor647-transferrin (K, L). The correlation between the fluorescence intensity ratio of the dipole potential sensitive indicator and the membrane microdomain marker is displayed in the figures. Quantitative evaluation of these dot plots is presented in Table 1.

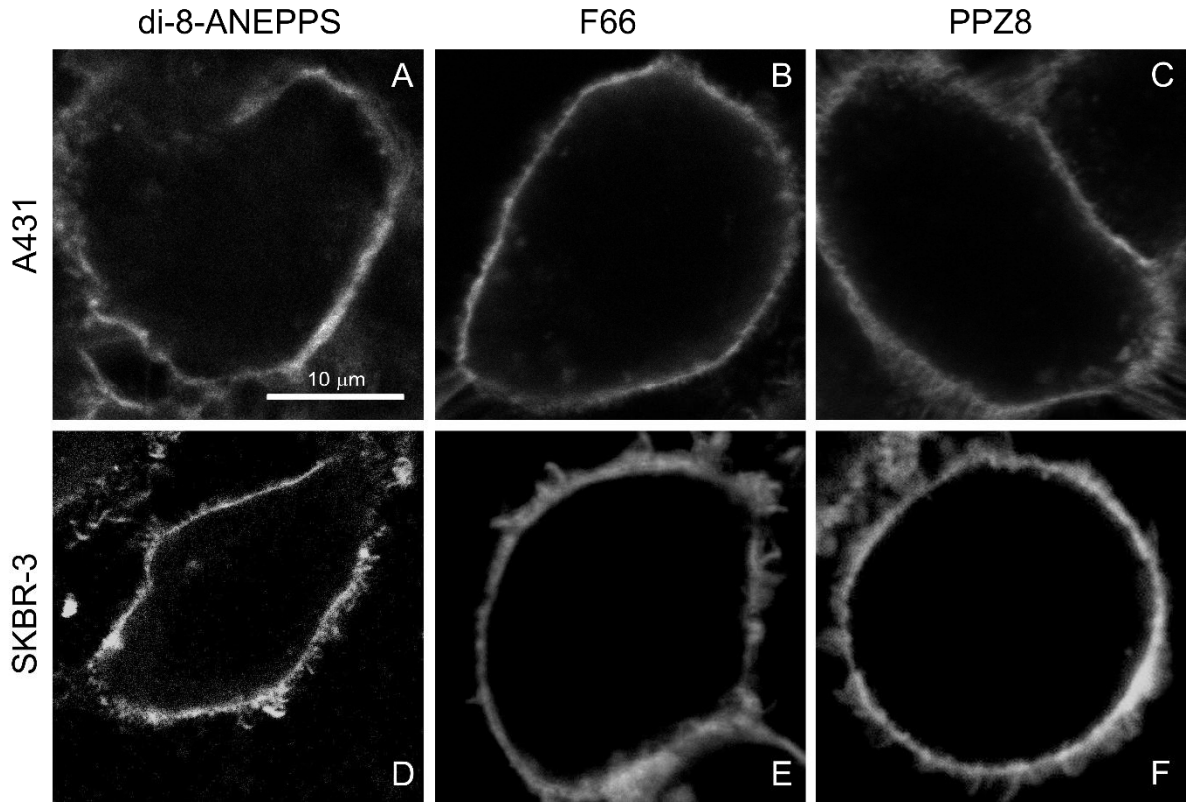

Supplemental Figure S3. Membrane localization of dipole potential-sensitive dyes. A431 (A-C) and SKBR-3 (D-F) cells were stained with di-8-ANEPPS (A, D), F66 (B, E) or PPZ8 (C, F) followed by recording confocal sections in the middle plain of cells.

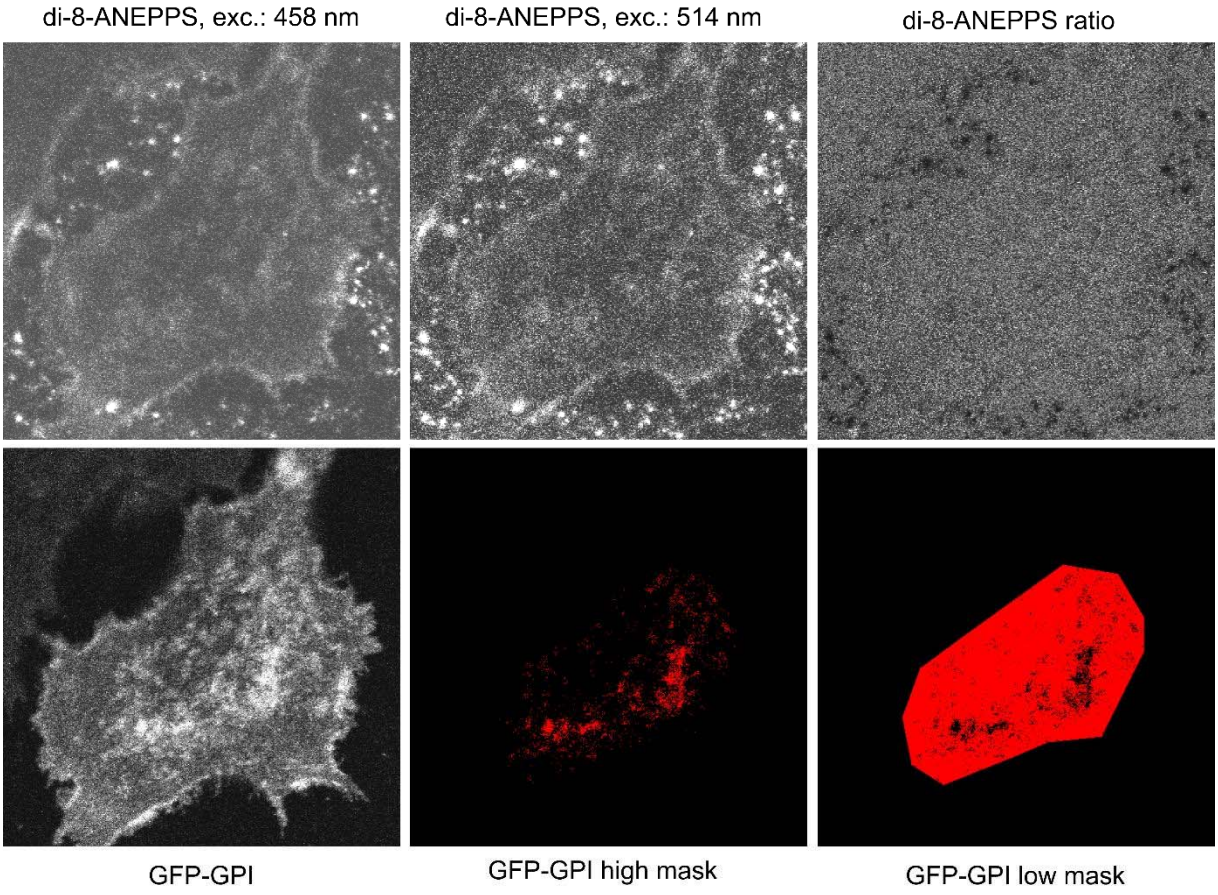

Supplemental Figure S4. Representative images showing the analysis of dipole potential inside and outside lipid rafts. SKBR-3 cells were transfected with GFP-GPI followed by staining them with di-8-ANEPPS two days after transfection. ANEPPS was excited at two different wavelengths (458 nm and 514 nm) and its emission was measured between 584 and 686 nm. The intensity recorded with an excitation of 458 nm was divided by that excited at 514 nm (di-8-ANEPPS ratio). The fluorescence of GFP-GPI was recorded in a third image which was segmented using the maxentropy algorithm. The intersection of the high intensity clusters identified by the segmentation and the cell mask drawn manually was considered to be the raft mask (GFP-GPI high mask). The intersection of the low intensity areas in the GPI-GPI image with the cell mask corresponds to the non-raft mask (GFP-GPI low mask). The di-8-ANEPPS ratio was evaluated in both masks separately.

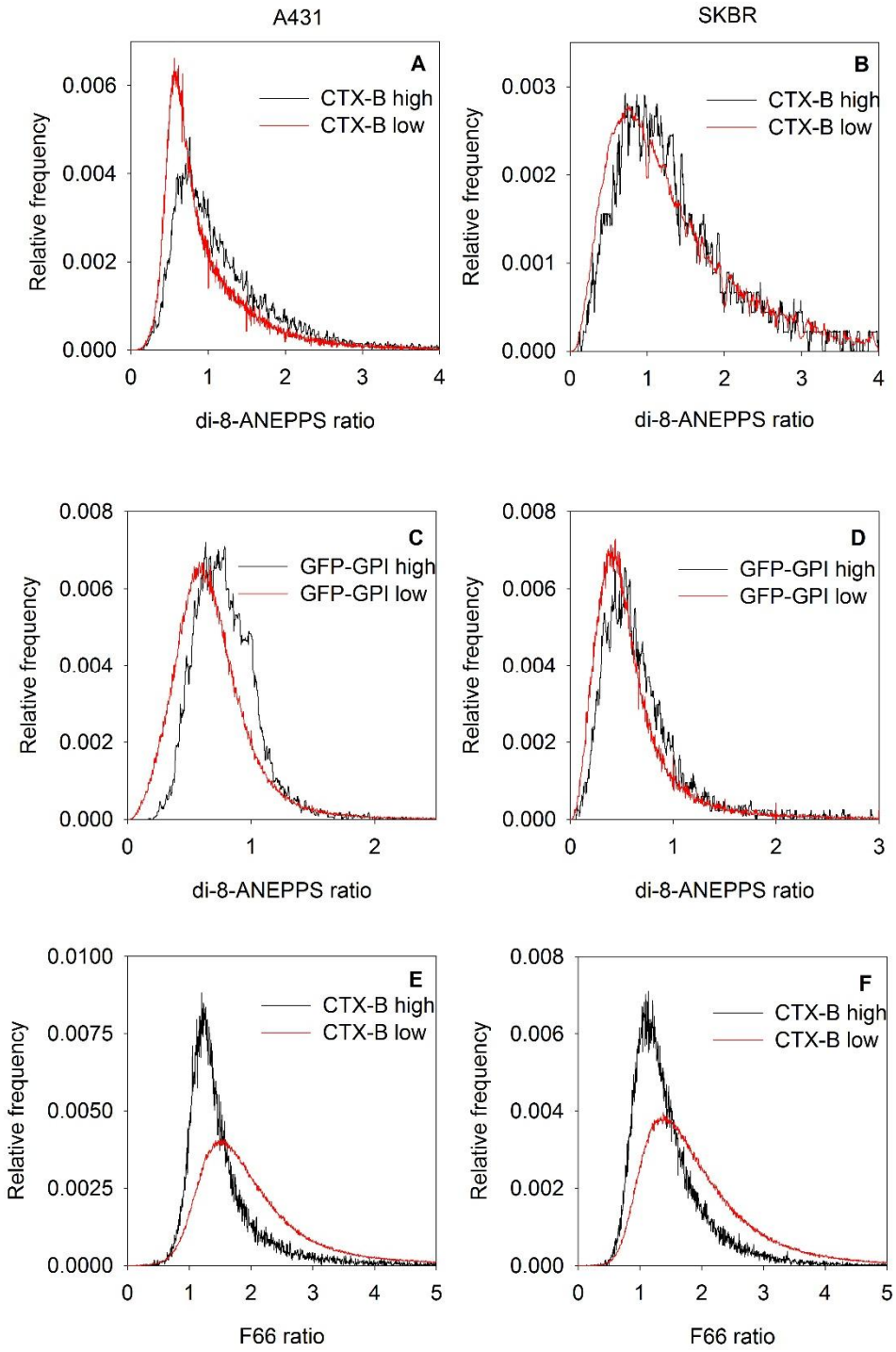

Supplemental Figure S5. The dipole potential inside and outside lipid rafts. A431 (A, C, E) and SKBR-3 (B, D, F) cells were labeled with the dipole potential sensitive dyes di-8-ANEPPS (A-D) or F66 (E, F). Lipid rafts were labeled with CTX-B staining (A, B, E, F) or GFP-GPI transfection (C, D). Images of the raft markers were segmented to produce raft and non-raft masks corresponding to high and low intensities of the raft markers, respectively, as shown in Fig. S3. The distribution of the di-8-ANEPPS excitation ratio and the F66 emission ratio was separately analyzed inside and outside lipid rafts, and their distributions are shown in the figures.

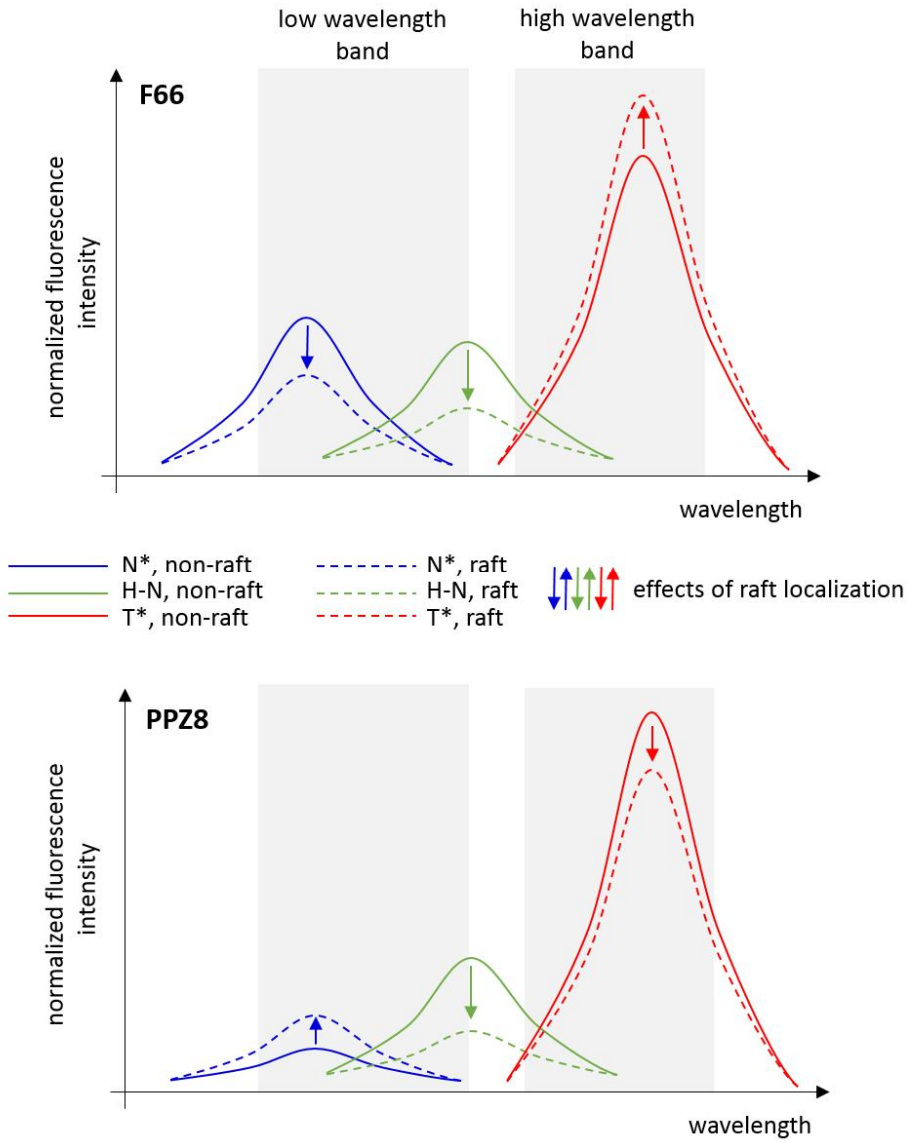

Supplemental Figure S6. Changes in the emission characteristics of 3-hydroxyflavone dyes in lipid rafts. The emission of 3-hydroxyflavone dyes originates from three different species. Species N* and T* interconvert by excited-state intramolecular proton transfer (ESIPT) and their ratio is sensitive to the dipole potential. The third species, H-N, is a hydrogen-bonded form of the dye. In the case of F66, the relative fraction of the N* species decreases upon increasing the dipole potential, while the opposite change occurs for PPZ8 due to the inverted orientation of the fluorophore. Lipid rafts not only exhibit a higher dipole potential, but also a more compact lipid structure resulting in less hydration of the membrane and a consequent decrease in the relative contribution of the H-N species to the emission and overall quenching of fluorescence from all three species. The effect of water quenching is not shown in the figure since the spectra are normalized to the total emission from the dye. Both the N* and H-N species contribute to the emission in the low wavelength range. Assuming the dipole potential is higher in lipid rafts than in the rest of the membrane the relative changes in the emission from the N* and H-N species change in the same direction for F66, but in the opposite direction for PPZ8. Therefore, the emission ratio of PPZ8, i.e. the fluorescence intensity in the low wavelength range vs. the high wavelength range, will not faithfully report the dipole potential difference between lipid rafts and non-raft regions.